COMPUTED POTENTIAL ENERGY SURFACES FOR CHEMICAL REACTIONS

Semi-Annual Report

for the period

July 1, 1992 - December 31, 1992

for
Cooperative Agreement NCC2-478

Submitted to

National Aeronautics and Space Administration
Ames Research Center
Moffett Field, California 94035

Computational Chemistry Branch
Dr. Stephen R. Langhoff, Chief and Technical Officer

Thermosciences Division
Dr. Jim Arnold, Chief

Prepared by

ELORET INSTITUTE
1178 Maraschino Drive
Sunnyvale, CA 94087
Phone: 408 730-8422 and 415 493-4710
Telefax: 408 730-1441

Dr. K. Heinemann, President and Grant Administrator
Dr. Stephen P. Walch, Principal Investigator
Dr. Eugene Levin, Co-Principal Investigator

22 January, 1993

(Initials)

ANALYTIC REVIEW FORM

Primary Record IPS # 141165

___ Document should not receive analytic treatment

SUBSIDIARY ADD

Document page range ____ to ____ New subsidiary # _____
Document page range ____ to ____ New subsidiary # _____
Document page range ____ to ____ New subsidiary # _____

SUBSIDIARY DELETE/CORRECTION

Subsidiary #_____
(IPS#_____)

___ Delete
Reason: ___ limited technical content
___ no separate authorship
___ context dependent

___ Adjust paging
___ Other _____

Subsidiary #_____
(IPS#_____)

___ Delete
Reason: ___ limited technical content
___ no separate authorship
___ context dependent

___ Adjust paging
___ Other _____

Subsidiary #_____
(IPS#_____)

___ Delete
Reason: ___ limited technical content
___ no separate authorship
___ context dependent

___ Adjust paging
___ Other _____

Investigator: Dr. Stephen Walch

A manuscript describing the calculations on the $^1CH_2 + H_2O$, $H_2 + HCOH$, and $H_2 + H_2CO$ product channels in the $CH_3 + OH$ reaction, which were described in the last progress report, has been accepted for publication in J. Chem. Phys., and a copy of the manuscript is included in the appendix. The production of $^1CH_2$ in this reaction is important in hydrocarbon combustion since $^1CH_2$ is highly reactive and would be expected to insert into N_2, possibly leading to a new source for prompt NO_x (vide infra).

The appendix also contains a copy of a paper (J. Chem. Phys., in press), which discusses the barriers for

$$H + CH_2O \leftrightarrow CH_3O \leftrightarrow CH_2OH$$

These species are also important in hydrocarbon combustion and the computed barrier heights are consistent with experimental work (F. Temps et al.) in contrast to earlier studies which obtained barrier heights which are too large.

During the last six months new calculations have been carried out for the $NH_2 + NO$ system, which is important in the thermal de-NO_x process. Fig. 1 shows a schematic of the computed potential energy surface (PES) for this system. Addition of NH_2 to NO leads to initial formation of an NH_2NO species (1). This species is found to be nonplanar, with a pyramidal geometry about the NH_2. Formation of $N_2 + H_2O$ proceeds via a complex series of steps starting with a 1,3-hydrogen shift to give a planar HNNOH species (2), in which the substituents are trans with respect to the NN bond and cis with respect to the NO bond. Rotation about the NO bond leading to (3) involves only a small barrier. However, rotation about the NN bond to give (4), which is the favorable configuration for elimination of H_2O, requires breaking an NN π bond and this pathway involves a very high barrier. Instead conversion of (3) and (4) is found to proceed via a planar saddle point which may be described as an inversion process. Subsequent elimination of H_2O occurs via a planar saddle point with an approximately rectangular arrangement of H-N-N-O. (See Fig. 2) The other product channel is HN_2

+ OH, which is expected to occur from (2), (3), or (4) with no barrier other than the exothermicity. Since the HN_2 + OH asymptote is at about the same energy as the bottle neck for formation of H_2O + N_2, the calculations suggest that both product channels are possible. An accurate estimate of the product branching ratio requires dynamics calculations (vide infra).

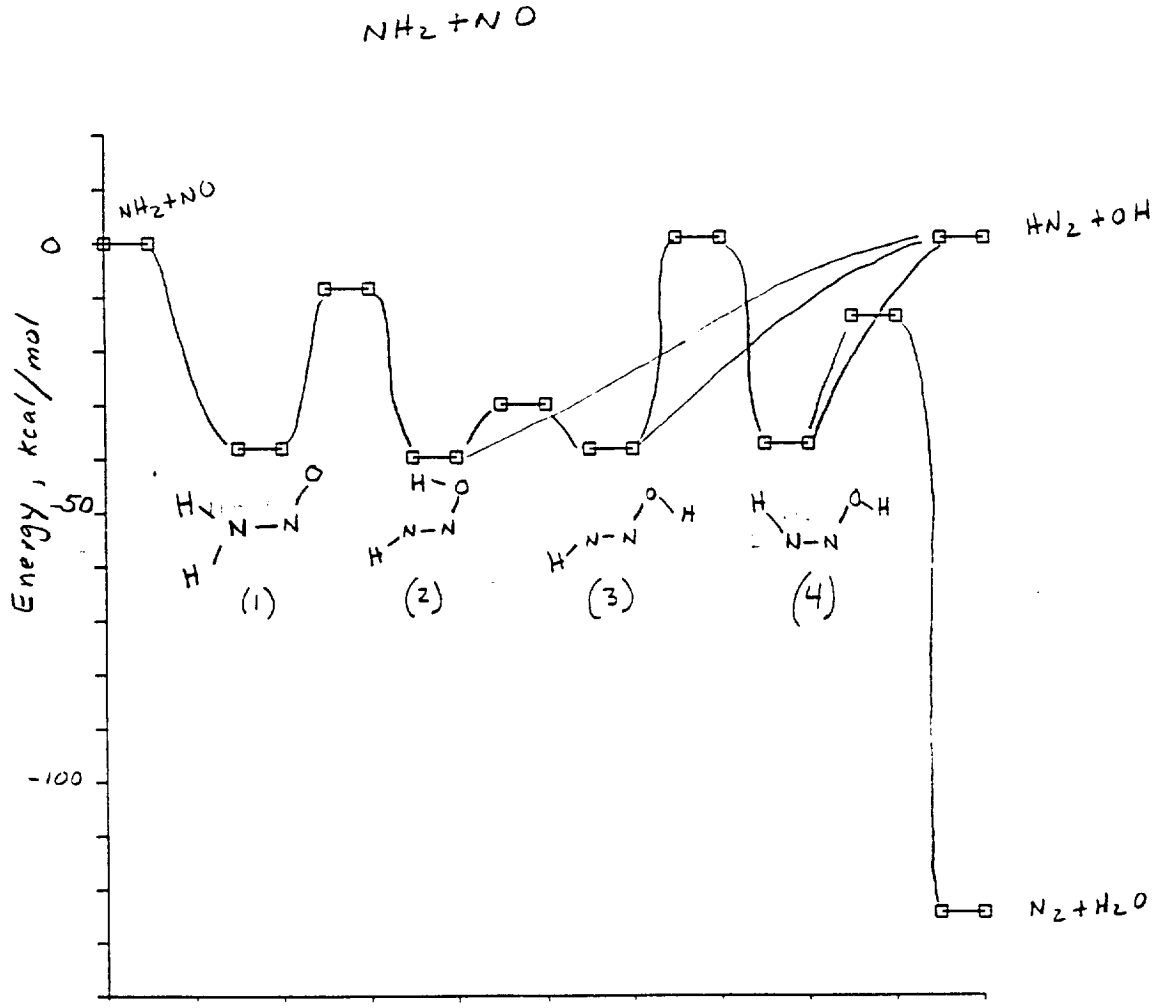

Fig. 1. Schematic of the PES for NH_2 + NO.

In a collaboration with Schatz (Northwestern) studies are being undertaken to determine the appropriate dynamics methods for determining product branching ratios in these complex reactions. As initial systems for study we have selected

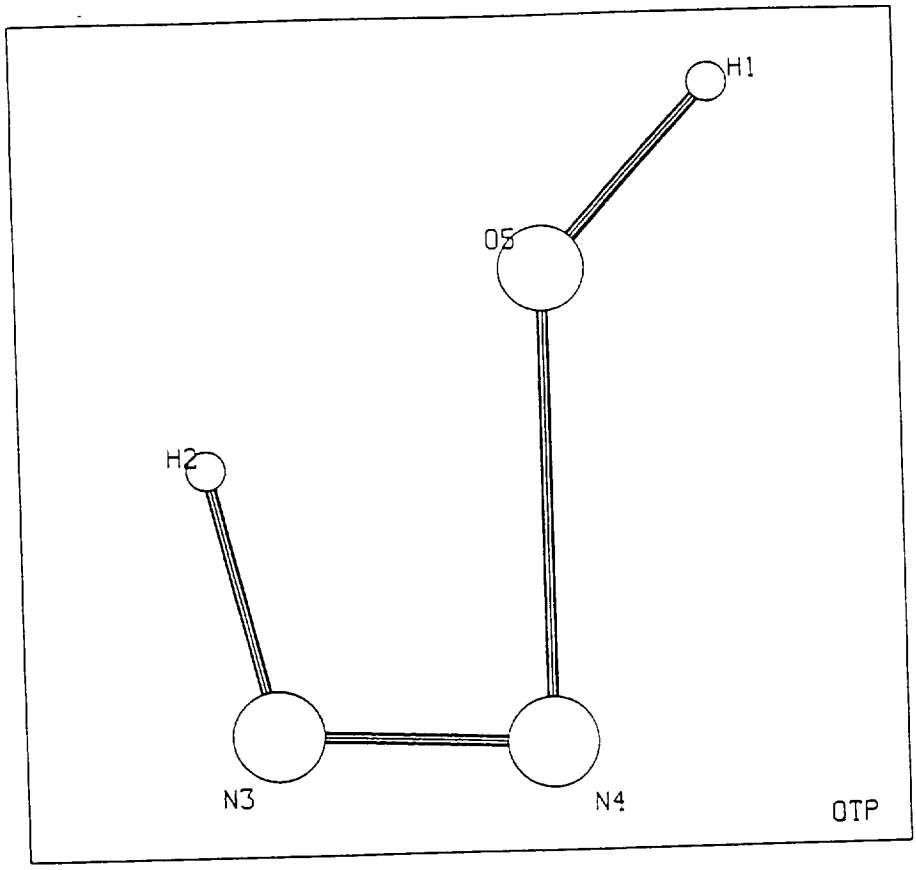

Fig. 2. Saddle point geometry for HNNOH (4) $\rightarrow H_2O + N_2$.

the HNO and HN + NO systems. In the first case the reaction to be studied is NH + O $\rightarrow$ N + OH or H + NO. Characterization of this system requires global PES's for the $^1A'$, $^3A''$, and $^1A''$ surfaces of H + NO. Current calculations on this system involve 19 values of the Jacobi angle, up to 10 values of R, and 4-6 values of r, or about 800 points to characterize the HNO and HON regions for three surfaces. Currently about 2/3 of the points have been completed. The global PES will be based on spline fits of the Morse parameters in r as was done previously for HN_2. It will also be necessary to represent the N + OH and NH + O channels, however, it is expected that this region of the surface can be represented with a simple functional form which requires few additional points. Once the surface is complete it will be possible to test various dynamical approximations.

For the NH + NO reaction, experiments have focused on H + NNO which leads

to NH + NO and N_2 + OH as major product channels. It is planned to spice together this surface from the known triatomic potentials (HNN, HNO, and NNO) plus information on the four atom system which is already available from work done previously under this grant (see the previous progress report). It is anticipated that a grid of points in the N_2 + OH region will also be needed to help characterize the portion of the surface involved in energy release. These studies should help to understand interesting experimental results (Wittig et al.) which show substantial internal energy (presumably vibrational energy) in the N_2 product.

In addition to continuation of the work discussed above future work will include studies of the $^1CH_2$ + N_2 reaction mentioned above. The initial product on the singlet surface is expected to be a cyclic CH_2N_2 isomer (C_{2v} symmetry). This species should have a fairly small bond energy (probably of the order of magnitude of 20 kcal/mol.). The cyclic isomer could open to form the singlet ground state of diazomethane or via a singlet-triplet surface crossing could lead to CH2N(doublet) + N(^{4}S). The latter process is expected to be endothermic by analogy to the isoelectronic reaction,

$$O(^1D) + N_2 \rightarrow NO + N(^4S) \tag{1}$$

which is endothermic by $\approx$ 30 kcal/mol. A more likely low barrier process is hydrogen abstraction from the initially formed cyclic CH_2N_2 to give a cyclic CHN_2 species (C_{2v} symmetry). This is the same species proposed by Yarkony in the analagous reaction

$$CH(^2\Pi) + N_2 \rightarrow HCN + N(^4S) \tag{2}$$

This process requires a singlet-triplet surface crossing, however, Yarkony's calculations show that the intersection of the two surfaces occurs at approximately the geometry of the cyclic CHN_2 species. In either case, the N atoms can enter into the second step of the thermal Zeldovich mechanism i.e.

$$N + O_2 \rightarrow NO + O \tag{2}$$

which leads to NO_x production. Initial work on this system will focus on the energetics of the species involved (i.e cyclic CH_2N_2, diazomethane, and CH_2N + $N(^4S)$). CH_2N if formed is expected to be highly reactive to O atoms formed by reaction (2). The expected products are $^1CH_2$ + NO. Thus, if production of CH_2N is an important pathway the $^1CH_2$ species serves a catalytic role in the net process

$$N_2 + O_2 \rightarrow 2NO \tag{3}$$

Another system which will be studied is H + HNO. This reaction may be important in experiments to simulate supersonic combustion where heated air is used resulting in formation of NO via the thermal (Zeldovich) process. Here HNO may be an intermediate in the recombination reaction

$$H + H + NO \rightarrow H_2 + NO$$

This system ties in with previous work on the NH_2O system and with current work on HNO.

Investigator: Dr. Eugene Levin

During the time period from 1 July 1992 to 31 December 1992, the determination of the transport properties of gases (e.g., viscosity, diffusion, thermal conductivity, etc.) from the collision cross-sections of the constituent species was completed for the mixtures H-H_2, H-H, H-Ar, and H-H_2O. This work was carried out in collaboration with NASA scientists Stallcop, Partridge (and others) and four papers documenting this work are in preparation for submission to the Journal of Chemical Physics.

The results for H-H_2O were particularly significant in three respects. Since the water molecule is in a C2V configuration rather than linear, a specific plane is determined. Hence, it was necessary to determine representative cross-sections for a very large number of collision approach directions between the hydrogen atom and the water molecule representing both in-plane angular variations as well as out-of-plane relative orientations. The only previous attempt to apply our method to other than binary collisions was a study of H-N_2 interactions ("H-N_2 interaction energies, transport cross sections, and collision integrals", by Stallcop, Partridge, Walch and Levin, JCP 97 (5), September 1992, pp. 3431-3436). That study did involve consideration of the various angles of approach, but since the N_2 molecule is linear, there was one less degree of freedom than in the case of H-H_2O. For water, over 50 different collision geometries were considered in order to obtain a reliable weighted mean cross section.

A second important aspect of the H-H_2O study was the discovery that the average cross-sections and collision integrals resulting from the weighted mean of the individual angular collision orientations differed very little from the results obtained by using an average potential energy representation. A similar result was found in the H-N_2 study cited above but it was unexpected for the more complex case of H-H_2O. If this proves to be a general result, it would simplify greatly the determination of cross sections and transport properties for interactions of atoms or ions with larger molecules. It may also apply for molecule-molecule collisions.

The third important feature of the H-H_2O study addressed the question of whether the semi-classical approximation used to calculate the phase shifts retained sufficient accuracy for small values of the reduced mass, μ, particularly at low energy levels. For H-H_2O the reduced mass is approximately 0.947 and energy levels as small as E=0.0001 hartrees were used in the study. The error in cross sections due to the semi-classical approximation was determined by direct integration of the radial Schroedinger equation to determine the phase shifts for a range of energy values using the average potential energy representation for the interaction of H with H_2O. It was found that the error in the cross sections diminished from about 12% at E=0.0001 to less than one percent at E=.002. The resulting error in the collision integrals decreased from about 4% at T=100 (Kelvin) to less than 1% at T=400 K. It was concluded that the semi-classical method remained valid except for extremely low energies and the correspondingly low temperatures.

As a result of the above findings for H-H_2O regarding the range of validity of the semi-classical method, all of our current work in the determination of cross sections and collision integrals now uses a quantum mechanical calculation for low energies and small reduced masses μ and only uses the semi-classical approximation above the energy level for which the difference is less than a fraction of 1%. Our earlier work on the transport properties of the constituents of air was rechecked to see if the limitations of the semi-classical method had resulted in erroneous results, however it was found that the published results were not affected since the reduced masses for interactions of O-O, N-N and N-O (and their ions) were much larger than collisions involving hydrogen. In all of these cases the differences between the semi-classical and quantum mechanical results were negligible.

Since the direct integration of the radial Schroedinger equation to obtain the quantum mechanically determined phase shifts is very time-consuming, a much more efficient method was developed by Schwenke which combines the techniques of R-matrix propagation and Richardson extrapolation. The algorithm is designated the HEMPR method (h-extrapolated Magnus propagator R-matrix). The details of this new algorithm will be contained in a joint paper by Levin,

Schwenke and Stallcop which compares the results of quantum mechanical and semi-classical determinations of cross sections and collision integrals for various energy levels and values of the reduced mass μ.

Since hydrogen is at least one of the collision partners, the reduced masses are small and consequently the results obtained for H-H, H-H_2, and H-Ar all were based on the HEMPR method at low energies and the semi-classical method after the differences became negligible. The results were found to be in quite good agreement with available highly accurate (but limited energy range) experiments. The extension of the cross section determination over a broad spectrum of energy levels permitted the transport properties to be presented over a wide range of temperatures of interest to NASA.

In addition to completing the documentation and publication of the work described above, the major goals of next time period are to undertake the study of molecule-molecule collisions (specifically, H_2-H_2, H_2-N_2, and N_2-N_2) and to complete an Air Reference Model. The molecule-molecule study is a significant advance over our prior atom-atom and atom-molecule work. Of particular interest will be to determine whether the average cross sections obtained by combining the cross sections for all the various possible collision orientations is or is not the same as the resulting cross sections using a mean potential. The completion of the Air Reference Model is awaiting the determination of the contributions from the collisions N-e^- and O-e^-.

Theoretical Characterization of the Reaction

$CH_3 + OH \rightarrow CH_3OH \rightarrow$ products :

The $^1CH_2 + H_2O$, $H_2 + HCOH$, and $H_2 + H_2CO$ Channels

Stephen P. Walch[a]
ELORET Institute
Palo Alto, Ca. 94303

Abstract. The potential energy surface (PES) for the CH_3OH system has been characterized for the $^1CH_2 + H_2O$, $H_2 + HCOH$, and $H_2 + H_2CO$ product channels using complete-active-space self-consistent-field (CASSCF) gradient calculations to determine the stationary point geometries and frequencies followed by CASSCF/ internally contracted configuration-interaction (CCI) calculations to refine the energetics. The $^1CH_2 + H_2O$ channel is found to have no barrier. The long range interaction is dominated by the dipole-dipole term, which orients the respective dipole moments parallel to each other but pointing in opposite directions. At shorter separations there is a dative bond structure in which a water lone pair donates into the empty a'' orbital of CH_2. Subsequent insertion of CH_2 into an OH bond of water involves a non-least-motion pathway. The $H_2 + HCOH$, and $H_2 + H_2CO$ pathways have barriers located at -5.2 kcal/mol and 1.7 kcal/mol, respectively, with respect to $CH_3 + OH$. From comparison of the computed energetics of the reactants and products to known thermochemical data it is estimated that the computed PES is accurate to $\pm$ 2 kcal/mol.

[a]Mailing Address: NASA Ames Research Center, Moffett Field, CA 94035.

I. Introduction

The CH_3 + OH reaction has at least six possible product channels:

$$CH_3 + OH + M \rightarrow CH_3OH + M \qquad (1a)$$

$$CH_3 + OH \rightarrow CH_2OH + H \qquad (1b)$$

$$CH_3 + OH \rightarrow CH_3O + H \qquad (1c)$$

$$CH_3 + OH \rightarrow^1 CH_2 + H_2O \qquad (1d)$$

$$CH_3 + OH \rightarrow HCOH + H_2 \qquad (1e)$$

$$CH_3 + OH \rightarrow H_2CO + H_2 \qquad (1f)$$

The role of reaction 1d has been controversial. The room temperature rate for the reverse of reaction 1d has been measured by Hatakeyama et al. [1] as $\approx 3 \times 10^{-12}$ cm^3 molecule^{-1}cm^{-1}, while Hack et al. [2] obtained 3.5×10^{-11} cm^3 molecule^{-1}cm^{-1}, or about an order of magnitude faster. The latter rate is approximately gas kinetic and implies no barrier. Using currently accepted heats of formation [3], and a singlet-triplet splitting for methylene of 9 kcal/mol, reaction 1d is exothermic by 0.7 kcal/mol at 0K. Thus, the forward reaction is also expected to be very fast.

Dean and Westmoreland [4] have used a variant of Rice-Ramsperger-Kassel-Marcus (RRKM) theory called QRRK theory to model the product distributions in the CH_3 + OH reaction. In this work the parameters for 1b and 1c were based on estimated rates for the reverse reaction. The parameters for reaction 1f were taken from calculations [5] and the rate for reaction 1d was taken from Ref. 1. According to these studies, at room temperature and moderate pressure CH_3OH is the dominant product, while at flame temperatures reaction 1b is thought to take

over. The HCOH + H_2 channel does not appear to have been considered in these studies, though theory [5] indicates essentially no barrier with respect to CH_3 + OH. This study indicated that production of $^1CH_2$ (reaction 1d) is a minor channel. By contrast a model proposed by Pilling and coworkers [6] which makes use of the rate for the reverse of reaction 1d due to Hack et al. [2] indicates that reaction 1d is the dominant channel above room temperature.

Recently Smith [7] has also reported RRKM calculations for CH_3 + OH. These calculations as well as the work of Pilling et al. [6] have indicated a need for more accurate potential energy surface (PES) information for the $^1CH_2$ + H_2O, H_2 + HCOH, and H_2 + H_2CO product channels. The most accurate previous theoretical study of these channels in the CH_3OH system was carried out by Harding, Schlegal, Krishnan, and Pople [5] using Møller-Plesset perturbation theory with a 6-311G** basis set. Although these calculations were carefully carried out, there is probably considerable uncertainty in the energetics; by current standards, both the basis set and treatment of electron correlation can be improved upon. More recently the bond dissociation energies of CH_3OH have been computed by Bauschlicher, Langhoff, and Walch [8] using the modified coupled-pair functional method. Similar calculations were carried out by Pople and co-workers [9] using the G2 method, which includes some empirical corrections. These calculations accurately determined the heats of formation of the CH_3O and CH_2OH species, but they did not consider the portions of the PES leading to the $^1CH_2$ + H_2O, H_2 + HCOH, and H_2 + H_2CO product channels. Thus, these regions of the PES are reexamined here.

Qualitative features of the potential energy surfaces are discussed in Sec. II, the computational method is discussed in Sec. III, the results are presented in Sec. IV, and the conclusions are given in Sec. V.

II. Qualitative Features.

CH_2 has two low-lying states. The $^3B_1$ ground state which will be drawn as:

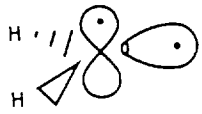

has two orthogonal high-spin coupled singly occupied orbitals, while the $^1A_1$ state, which is $\approx$ 9 kcal/mol higher, is drawn as:

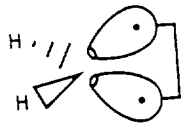

i.e., the two orbitals corresponding to the C lone pair are singlet paired. If these orbitals are solved for self consistently in a generalized valence bond wavefunction [10] the overlap integral between them is ≈ 0.7. Thus, the singlet state of CH_2 may be characterized as a singlet biradical, but the orbitals of the lone pair have a substantial overlap, which must be maintained while inserting into a single bond if the process is to occur without a substantial barrier. In terms of multiconfigurational self-consistent-field (MCSCF) theory, the biradical character in CH_2 arises because of a near degeneracy effect between an sp hybrid lone pair and an empty 2p-like a'' orbital.

The insertion of $^1CH_2$ into a bond pair occurs via a non-least-motion pathway. This process is completely analagous to the non-least-motion addition of the $^2\Pi$

state of CH to H_2, as discussed by Dunning and Harding [10]. In that case the CH and H_2 approach each other with the bond axes parallel and for this orientation the C lone pair and H_2 bond pair orbitals are able to evolve into two CH bonding orbitals without breaking either bond. These orbital changes are consistent with the orbital phase continuity principle arguments made by Goddard [11].

In the case of $^1CH_2 + H_2O$ the long range interaction is dominated by the dipole-dipole term, which leads to an initial approach with the dipoles parallel to each other but pointed in the opposite direction. At shorter separation there is a dative bonded structure where one lone pair on H_2O donates into the empty C 2p-like orbital of CH_2. This structure is a minimum on the PES. Insertion of CH_2 into one of the H_2O bonds requires rotating H_2O such that one OH bond is in the plane defined by O and the bisector of $\angle$ HCH. This orientation is similar to the orientation favored for non-least-motion insertion of CH into H_2.

Insertion of $^1CH_2$ into H_2O involves very little barrier. The insertion of hydroxy methylene (HCOH) into H_2, however, is found to exhibit a barrier of 13.9 kcal/mol. The lower reactivity of HCOH as compared to CH_2 results from delocalization of an O lone pair into the empty C 2p orbital. The resultant exclusion effect reduces the 2s $\rightarrow$ 2p near-degeneracy effect and thus results in less biradical character in the substituted carbene.

III. Computational Details.

Two different basis sets were used in this work. For the CASSCF gradient calculations the polarized double-zeta set of Dunning and Hay [12] was used. The basis set for C and O is a (9s5p)/[3s2p] basis augmented by a single set of 3d functions with exponents of 0.75 and 0.85 for C and O, respectively. The H basis is (4s)/[2s] augmented with a single set of 2p functions with exponent 1.00. The basis set used in the CI calculations is the Dunning correlation consistent triple-zeta double-

polarization basis set [13]. This basis is [4s3p2d1f] for C and O and [3s2p1d] for H and is described in detail in Ref. 13.

In the CASSCF calculations the electrons in the bonds which are being made or broken were included in the active space. In the case of the $^1CH_2 + H_2O$ and $H_2CO + H_2$ channels, there were six active electrons and six active orbitals. The correlated electrons correspond to the CO bond, the OH bond, and one CH bond of CH_3OH and evolve to the C lone pair of CH_2 and the two OH bond pairs in the case of $^1CH_2 + H_2O$ and the CO σ and π bonds and the H_2 bond in the case of $H_2CO + H_2$. The remaining 12 electrons are inactive in the CASSCF calculation. In the case of the $HCOH + H_2$ channel, there were four active electrons and four active orbitals. The correlated electrons correspond to two CH bonds in CH_3OH and to the C lone pair in HCOH and the H_2 bond pair in the $HCOH + H_2$ limit. The remaining 14 electrons were inactive in the CASSCF calculation. In generating the set of reference configurations, no more than two electrons were permitted in the weakly occupied CASSCF orbitals. All but the O 1s and C 1s electrons were correlated in the CCI calculations.

The CASSCF/gradient calculations used the SIRIUS/ABACUS system of programs [14], while the CCI calculations were carried out with MOLPRO [15,16]. Most of the calculations were carried out on the NASA Ames Cray Y-MP; although some of the CCI calculations were carried out on the NAS facility Y-MP.

IV. Discussion.

Table I shows computed energetics for the portions of the CH_3OH surface which were considered in this work. The computed energetics were obtained from the CCI energies (including the multireference analogue of the Davidson correction [17]) plus the zero-point energies from the CASSCF calculations. (See Tables IIa-IIc.) Thus, these energetics should be compared to experimental values at 0 K. The computed

frequencies and rotational constants for the saddle points for $CH_2O + H_2$, HCOH + H_2, and $^1CH_2 + H_2O$, (denoted as CH_2O-H_2, HCOH-H_2, and CH_2-H_2O, respectively) and for the $CH_2 + H_2O$ dative bonded structure (denoted as $CH_2.H_2O$) are also given in Table III. The stationary point corresponding to $CH_2.H_2O$ is a minimum on the PES, but there is one very small frequency (26 cm^{-1}), which corresponds to a hindered rotation of the CH_2 and H_2O with respect to each other.

The computed energy separations discussed here, in each case, involve breaking two bonds and forming two new bonds; thus, the errors in the individual bond strengths cancel and the computed energetics are expected to be accurate. However, in Ref. 2 it was shown that, for calculations of about the same quality as reported here, the error in the C-O bond strength in CH_3OH is 6.5 kcal/mol. Thus, in order to compute energies with respect to $CH_3 + OH$, the experimental 0 K value of 90.2 kcal/mol [18] was used for the C-O bond strength. The locations of the H + CH_3O and H + CH_2OH asymptotes were taken as the best-estimate values from Ref. 2. This places H + CH_3O and H + CH_2OH at 14.8 kcal/mol and 6.0 kcal/mol above $CH_3 + OH$, respectively. The experimental locations of $^1CH_2 + H_2O$ and CH_2O + H_2 with respect to CH_3OH were derived from the JANAF [3] heats of formation of H_2, CH_2O, CH_3, OH, H_2O(g), and $^3CH_2$, plus a singlet-triplet splitting in CH_2 of 9.0 kcal/mol and the value for the C-O bond strength in CH_3OH given above.

From Table I it is seen that the computed $CH_3OH \rightarrow {}^1CH_2 + H_2O$ separation is 0.7 kcal/mol smaller than experiment, while the computed $CH_3OH \rightarrow CH_2O$ + H_2 separation is 0.6 kcal/mol smaller than experiment. It is also seen that the computed results of Harding et al. [5] are 5.4 kcal/mol larger and 2.3 kcal/mol smaller, respectively, for the same separations. The computed barrier heights for $CH_3OH \rightarrow$ HCOH + H_2 and $CH_3OH \rightarrow CH_2O + H_2$ obtained in Ref. 5 are 6.0 kcal/mol and 4.6 kcal/mol larger than the barrier heights obtained in the present

work. These differences presumably reflect a combination of the larger basis set and more extensive correlation treatment in the present calculations. Based on the comparison to experiment for the $^1CH_2 + H_2O$ and $CH_2O + H_2$ asymptotes it is reasonable to assign error bars of $\approx \pm 2$ kcal/mol to the computed energetics in this work.

The computed energetics for the CH_3OH system are also shown schematically in Fig. 1. From Fig. 1 it is seen that only the $CH_2O + H_2$ channel exhibits a barrier (1.7 kcal/mol.) with respect to $CH_3 + OH$. The $H_2 + HCOH$ channel has a barrier, but it is below $CH_3 + OH$. The $^1CH_2 + H_2O$ channel has no barrier and is computed to be 1.4 kcal/mol below $CH_3 + OH$. The $CH_3O + H$ and $CH_2OH + H$ channels are endoergic with respect to $CH_3 + OH$, but no intermediate barriers are expected. Thus, from this work the $^1CH_2 + H_2O$, $HCOH + H_2$, and $CH_2O + H_2$ channels are all found to be accessible from $CH_3 + OH$.

Fig. 2 shows the energy as a function of r_{CO} for the addition of $^1CH_2$ to H_2O, while the computed energies are given in Table IV. Two stationary points have been located along this minimum energy path. At long r_{CO} the dominant interaction is dipole-dipole, which results in an orientation with the dipole moments of the approaching molecules parallel to each other but pointing in opposite directions, as illustrated in Fig. 2. At shorter r_{CO} there is a minimum on the PES with C_s symmetry, followed by a saddle point with no symmetry for insertion of $^1CH_2$ into an OH bond of water. In order to characterize the minimum energy path, a gradient calculation was carried out starting at the saddle point and proceeding toward the minimum. CCI calculations were then carried out at the geometries corresponding to each step on the walk. This calculation defines the minimum energy path between the saddle point and minimum. It is not possible to do the same calculation for the portion of the PES connecting the minimum and the $^1CH_2$

+ H_2O asymptote, since there is no well-defined way to follow the gradient uphill. In order to characterize this portion of the PES, calculations were carried out with the CH_2 and H_2O molecules fixed at their equilibrium geometries and oriented with the planes of the molecule parallel to each other and the CO bond perpendicular to both molecular planes in the orientation shown in Fig. 2. For this geometric orientation, r_{CO} was varied and the resulting energies at the CCI level are also included in Fig. 2.

The main features of Fig. 2 are a shallow minimum followed by a small barrier to formation of CH_3OH. However, the barrier is below the $^1CH_2$ + H_2O asymptote and therefore the bottleneck on the vibrationally adiabatic curve is expected to occur in the entrance channel region. The main feature responsible for the entrance channel bottleneck is the building in of bending modes, which arise from electrostatic (dipole-dipole, dipole-quadrapole, and quadrapole-quadrapole) interactions. In order to define this interaction, dipole and quadrapole moments (about the center of mass) were computed for $^1CH_2$ and H_2O and are given in Table V. The experimental values [19] for H_2O (in a.u.) are $\mu = 0.73$, $Q_{xx} = 1.955$, Q_{yy} = -1.859, and Q_{zz} = -0.097; which are in reasonable agreement with the computed values.

V. Conclusions.

The potential energy surface (PES) for the CH_3OH system has been characterized for the $^1CH_2$ + H_2O, H_2 + HCOH, and H_2 + H_2CO product channels using complete-active-space self-consistent field (CASSCF) gradient calculations to determine the stationary point geometries and frequencies followed by CASSCF/ internally contracted configuration-interaction (CCI) calculations to refine the energetics.

The H_2 + H_2CO, and H_2 + HCOH pathways have barriers located at 1.7 kcal/mol and - 5.2 kcal/mol with respect to CH_3 + OH. The $^1CH_2$ + H_2O channel is found to

have no barrier in the absence of vibrational zero-point effects. However, the long range-interaction is dominated by a dipole-dipole term and the zero-point effects due to this interaction are expected to lead to a bottleneck on the vibrationally adiabatic minimum energy path. The $^1CH_2 + H_2O$ asymptote is computed to be 1.4 kcal/mol below $CH_3 + OH$. Thus, all three of these channels are expected to be accessible at moderate temperatures.

From comparison of the computed energetics of the reactants and products to known thermochemistry it is estimated that the computed PES is accurate to $\pm$ 2 kcal/mol.

Acknowledgement. SPW was supported by NASA cooperative agreement number NCC2-478.

References

1. S. Hatakeyama, H. Bandow, M. Okuda, and H. Akimoto, J. Phys. Chem., **85**, 2249(1981).
2. W. Hack, H.Gg. Wagner, and A. Wilms, Ber. Bunsen-Ges. Phys. Chem. **92**, 620(1988).
3. M.W. Chase, Jr.,C.A. Davies, J.R.Downey, Jr., D.J. Frurip, A.A. McDonald, and A.N. Syverud, J. Phys. Chem. Ref. Data, **14**, Suppl. 1(1985).
4. A.M. Dean and P.R. Westmoreland, Int. J. Chem. Kinet., **19**, 207(1987).
5. L.B. Harding, H.B. Schlegal, R. Krishnan, and J.A. Pople, J. Phys. Chem., **84**, 3394(1980).
6. N.J. Green, A.R. Pereira, M.J. Pilling, and S.H. Robinson, presented at the 23rd Symposium (International) on Combustion, 1990; poster.
7. G.P. Smith, 203rd ACS National Meeting, San Francisco, April 1992.
8. C.W. Bauschlicher, Jr., S.R. Langhoff, and S.P. Walch, J. Chem. Phys., **96**, 450(1991).
9. L.A. Curtiss, L.D. Kock, and J.A. Pople, J. Chem. Phys., **95**, 4040(1991).
10. T.H. Dunning Jr. and L.B. Harding, Theory of Chemical Reaction Dynamics, M. Baer ed, CRC Press, Boca Raton, Florida, 1985, pp. 1-69.
11. W.A. Goddard III, J. Amer. Chem. Soc., **94**, 793(1972).
12. T.H. Dunning,Jr and P.J. Hay in Methods of Electronic Structure Theory, H.F. Schaefer III ed., Plenum Publishing, 1977
13. T.H. Dunning Jr., J. Chem. Phys., **90**, 1007(1989).
14. SIRIUS is an MCSCF program written by H.J. Jensen and H. Agren and ABACUS is an MCSCF derivatives program written by T. Helgaker, H.J.

Jensen, P. Jørenson, J. Olsen, and P.R. Taylor.

15. H.-J. Werner and P.J. Knowles, J. Chem. Phys., **89**, 5803(1988).

16. P.J. Knowles and H.-J. Werner, Chem. Phys. Lett., **145**, 514(1988).

17. S.R. Langhoff and E.R. Davidson, Int. J. Quantum Chem,, **8**, 61(1974).

18. D.D. Wagman, W.H. Evans, V.B. Parker, S.H. Schumm, I. Halow, S.M. Bailey, K.L. Churney, and R.L. Nutall, J. Phys. Chem. Ref. Data, **11**, Suppl. 1(1982).

19. C.G. Gray and K.E. Gubbins, Theory of Molecular Fluids, Vol. I, Clarendon Press, Oxford (1984).

Table I. Computed Energetics for CH_3OH[a,b]

	calc.	exp(0K)	Harding et al.
$CH_3 + OH$		90.2	
$HCOH\text{-}H_2$	85.0		91.0
$HCOH + H_2$	71.1		71.1
$^1CH_2 + H_2O$	88.8	89.5[c]	94.9
$CH_2O\text{-}H_2$	91.9		96.5
$CH_2O + H_2$	18.1	18.7	16.4
CH_3OH	0.0	0.0	0.0

[a] CASSCF/CCI with a [4s3p2d1f/3s2p1d] basis set.

[b] Relative energies in kcal/mol (including zero-point energy).

[c] Using $^3CH_2 \rightarrow {}^1CH_2$ separation of 9.0 kcal/mol.

Table IIa. Computed energies and zero-point corrections.

$$CH_3OH \rightarrow CH_2O + H_2$$

	Energy[a]	zero-point energy[b]	Δ E[c]
CH_3OH	-115.51397(-.54566)	0.05258	0.0
CH_2O-H_2	-115.35603(-.39071)	0.04407	91.9
CH_2O+H_2	-115.47215(-.50189)	0.03768	18.1

[a] Energy in E_H. The first energy is the CCI energy, while the energy in parenthesis includes a multi-reference Davidson correction and is with respect to -115. E_H.

[b] zero-point energy in E_H.

[c] relative energy in kcal/mol including zero-point energy and a multi-reference Davidson's correction.

Table IIb. Computed energies and zero-point corrections.

$$CH_3OH \rightarrow^1 CH_2 + H_2O$$

	Energy[a]	zero-point energy[b]	Δ E[c]
CH_3OH	-115.51397(-.54566)	0.05258	0.0
CH_2-H_2O	-115.36931(-.40561)	0.04366	82.3
CH_2+H_2O	-115.35989(-.39040)	0.03884	88.8

[a] Energy in E_H. The first energy is the CCI energy, while the energy in parenthesis includes a multi-reference Davidson correction and is with respect to -115. E_H.

[b] zero-point energy in E_H.

[c] relative energy in kcal/mol including zero-point energy and a multi-reference Davidson's correction.

Table IIc. Computed energies and zero-point corrections.

$$CH_3OH \rightarrow HCOH + H_2$$

	Energy[a]	zero-point energy[b]	Δ E[c]
CH_3OH	-115.50589(-.54231)	0.05258	0.0
HCOH-H_2	-115.35803(-.39640)	0.04225	85.0
HCOH+H_2	-115.37823(-.41465)	0.03828	71.1

[a] Energy in E_H. The first energy is the CCI energy, while the energy in parenthesis includes a multi-reference Davidson correction and is with respect to -115. E_H.

[b] zero-point energy in E_H.

[c] relative energy in kcal/mol including zero-point energy and a multi-reference Davidson's correction.

Table III. Computed saddle point frequencies and rotational constants(cm^{-1}).

	CH_2O-H_2	HCOH-H_2	CH_2.H_2O	CH_2-H_2O
ω_1	3195	4130	3860	3723
ω_2	2295	3199	3744	3319
ω_3	1740	2323	3187	3222
ω_4	1574	1564	3113	2091
ω_5	1429	1498	1691	1560
ω_6	1369	1347	1515	1524
ω_7	916	1291	802	1119
ω_8	$2877i$	1122	610	949
ω_9	3278	934	337	703
ω_{10}	1273	622	334	438
ω_{11}	1211	513	161	387
ω_{12}	1065	$1414i$	26	$1850i$
A	3.345	3.042	4.117	4.640
B	0.944	0.839	0.358	0.496
C	0.863	0.764	0.349	0.478

Table IV. Computed energies and zero-point corrections[a].

$$CH_2 + H_2O \rightarrow CH_2 - H_2O$$

r_{CO}	CAS Energy	CI Energy[b]	zero-point energy	total[c]
3.834	-115.00924	-115.36931(-.40561)	0.04366	(-.36225)
3.929	-115.01305	-115.36889(-.40409)	0.04449	(-.35960)
4.076	-115.01765	-115.36968(-.40420)	0.04550	(-.35870)
4.207	-115.02142	-115.37055(-.40452)	0.04546	(-.35906)
4.310	-115.02426	-115.37130(-.40480)	0.04523	(-.35957)
4.386	-115.02635	-115.37189(-.40503)	0.04500	(-.36003)
4.437	-115.02785	-115.37230(-.40516)	0.04482	(-.36034)
4.471	-115.02890	-115.37254(-.40517)	0.04470	(-.36047)
4.528	-115.03024	-115.37237(-.40450)	0.04421	(-.36029)
5.0	-115.02970	-115.36971(-.40136)		
5.5	-115.02892	-115.36727(-.39843)		
6.0	-115.02797	-115.36541(-.39630)		
6.5	-115.02710	-115.36400(-.39475)		
7.0	-115.02635	-115.36294(-.39358)		
8.0	-115.02526	-115.36151(-.39206)		
9.0	-115.02464	-115.36076(-.39127)		
10.0	-115.02433	-115.36040(-.39091)		

[a] All energies in E_H. r_{CO} is in a. u.

[b] The first energy is the CCI energy, while the energy in parenthesis includes a multi-reference Davidson correction and is with respect to -115. E_H.

[c] Energy with respect to -115. E_H. The energy includes the zero-point correction and a multi-reference Davidson correction.

Table V. Computed dipole and quadrapole moments [a].

	μ	Q_{xx}	Q_{yy}	Q_{zz}
H_2O	0.768	-1.987	1.955	0.032
CH_2 $^1A_1$	0.679	1.187	0.496	-1.683

[a] Properties are in a.u. Quadrapole moment is with respect to the center of mass. The molecule is in the YZ plane with the C_2 axis in the Z direction.

Figure Captions.

Fig. 1. Schematic diagram of the potential energy surface for CH_3 + OH. The location of the CH_3 + OH asymptote with respect to CH_3OH is taken from experiment, while the locations of the CH_2OH + H aand CH_3O + H asymptotes are from previous calculations.

Fig. 2. The potential for $^1CH_2$ + H_2O from CCI calculations along the CASSCF minimum energy path. See the text.

Fig. 1

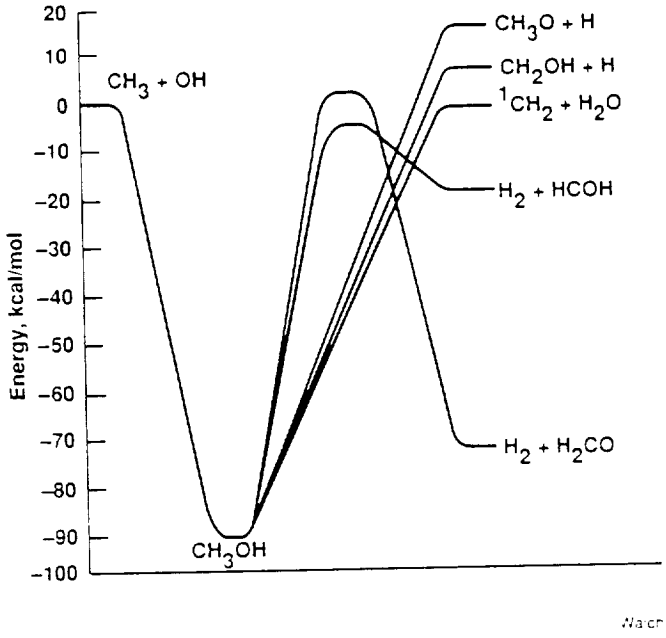
20
10
0
−10
−20
−30
−40
−50
−60
−70
−80
−90
−100
Energy, kcal/mol
CH3 + OH
CH3OH
CH3O + H
CH2OH + H
1CH2 + H2O
H2 + HCOH
H2 + H2CO

Fig. 2

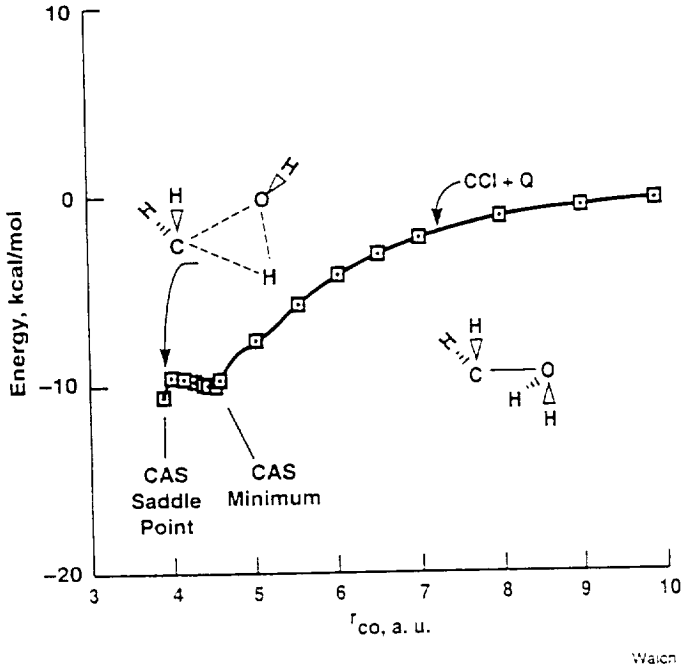
10
0
−10
−20
Energy, kcal/mol
3
4
5
6
7
8
9
10
r_{CO}, a. u.
CCl + O
CAS
Saddle
Point
CAS
Minimum
H
C
O
H
H
H
C
O
H
H
Walch

Computed Barrier Heights for

$H + CH_2O \leftrightarrow CH_3O \leftrightarrow CH_2OH$

Stephen P. Walch[a]
ELORET Institute
Palo Alto, Ca. 94303

Abstract. The barrier heights (including zero-point effects) for $H + CH_2O \rightarrow CH_3O$ and $CH_3O \rightarrow CH_2OH$ have been computed using complete active space self consistent field (CASSCF)/ gradient calculations to define the stationary point geometries and harmonic frequencies and internally contracted configuration-interaction (CCI) to refine the energetics. The computed barrier heights are 5.6 kcal/mol and 30.1 kcal/mol, respectively. The former barrier height compares favorably to an experimental activation energy of 5.2 kcal/mol.

The CH_3O radical is important in combustion and atmospheric chemistry [1]. In addition, recent experiments have studied individual rovibrational states of CH_3O above the H-CH_2O dissociation threshold by stimulated emission pumping [3]. The interpretation of these experiments depends critically on the barriers to decomposition of CH_3O to H + CH_2O and rearrangment to CH_2OH. Previous studies of these barrier heights include the work of Saebø, Radom, and Schaefer [2], who used Møller-Plesset perturbation theory through third order with small basis sets up through 6-31G**. More recently, Page, Lin, He, and Choudhury [4] reported somewhat more accurate calculations using multireference configuration-interaction (MRCI) with polarized triple zeta basis sets. In the present paper more accurate calculations are reported which make use of larger basis sets and extensive CI.

Two different basis sets were used in this work. For the complete active space self consistent field (CASSCF) gradient calculations the polarized double zeta set of Dunning and Hay [5] was used. The basis set for C and O is a (9s5p)/[3s2p] basis augmented by a single set of 3d functions with exponents of 0.75 and 0.85 for C and O, respectively. The H basis is (4s)/[2s] augmented with a single set of 2p functions with exponent 1.00. The basis set used in the CI calculations is the Dunning correlation consistent triple zeta double polarization basis set [6]. This basis is [4s3p2d1f] for C and O and [3s2p1d] for H and is described in detail in Ref. 6.

The calculations were carried out in C_s symmetry for a wavefunction of $^2A'$ symmetry. From the Hessian matrix in the diagonal representation, the stationary points obtained in C_s symmetry are the minimum for CH_2O + H, the saddle point for CH_2O + H $\rightarrow$ CH_3O, the CH_3O minimum, and the saddle point for $CH_3O \rightarrow CH_2OH$. For CH_3O the $^2A'$ state corresponds to one component of the ^2E state in C_{3v} symmetry. According to the calculations of Saebø et al. [2], the Jahn-Teller stabilization energy in this system is 0.56 kcal/mol and the Jahn-Teller splitting is 0.12 kcal/mol, with the $^2A'$ component lower. CH_2OH is found to have no symmetry and the use of a mirror plane of symmetry would not be appropriate. However, the separation between CH_3O and CH_2OH has been accurately computed by Bauschlicher, Langhoff, and Walch [7] and further calculations for CH_2OH were not carried out here.

The CASSCF calculations consisted of five electrons and five orbitals. The active electrons for CH_3O included the CO bond pair, one CH bond pair (the CH bond in the molecular plane), and the a' O 2p like orbital. These orbitals correspond to the CO σ and π bonds plus a H 1s orbital for CH_2O + H. The remaining electrons, which are inactive, include the other two CH bond pairs, the a'' O 2p like orbital and the O 1s, O 2s, and C 1s like orbitals. In generating the set of reference configurations for the subsequent internally contracted CI (CCI) calculations, no more than two electrons were permitted in the weakly occupied CASSCF orbitals. All but the O 1s and C 1s electrons were correlated in the CCI calculation. A multi-reference analog of Davidson's correction [8] was added to the CCI energies.

The CASSCF/gradient calculations used the SIRIUS/ABACUS system of programs [9], while the CCI calculations were carried out with MOLPRO [10,11]. The calculations were carried out on the NASA Ames Cray Y-MP.

Table I gives the harmonic vibrational frequencies, rotational constants, and geometric parameters for the stationary points considered in this work. Here H_a is the H of the spectator CH bonds, while H_b is the hydrogen which transfers during the reaction. The geometries and frequencies in Table I are quite similar to those obtained by Page et al. [4]. This is expected since a CASSCF wavefunction was used in Ref. 4. However, in Ref. 4 the CO σ bond was not correlated. For CH_3O this has the expected effect that the CO bond is elongated by ≈ 0.03 Å compared to the calculations in Ref. 4. At the H-CH_2O saddle point the CO bond is elongated by ≈ 0.02 Å and the C-H_b bond is shorter by ≈ 0.05 Å as compared to Ref 4. There are larger differences between this work and the results of Saebø et al. Here the geometry for CH_3O is similar except for the expected elongation of the C-H_b and CO bonds. However, there are significant differences in the geometry of the H-CH_2O saddle point. In particular, the C-H_b bond length is shorter by ≈ 0.18 Å . This result is consistent with the expectation that saddle point geometries will be more sensitive to electron correlation effects than will stationary points.

Table II gives the computed energies and zero-point corrections. The energies are from the CCI calculations, while the zero-point corrections are derived from the CASSCF harmonic frequencies. From Table II it is seen that the relative energies are only very slightly changed (≈ 0.1 kcal/mol) in going from the [4s3p2d1f/3s2p1d]

basis set to the [5s4p3d2f/4s3p2d] basis set. Table III compares the computed barrier heights obtained in the present calculations to those obtained by Saebø et al. [2] and by Page et al. [4]. Here it is seen that the barriers obtained by Saebø et al. are too large by $\approx$ 6 kcal/mol., while the barrier for $H + CH_2O \rightarrow CH_3O$ obtained by Page et al. is 2.3 kcal/mol larger than in the present calculations. Our computed barrier height is 5.6 kcal/mol for $H + CH_2O \rightarrow CH_3O$ and 5.2 kcal/mol for $D + CH_2O \rightarrow CDH_2O$. This result is in good agreement with experimental estimated activation energies of 5.2 kcal/mol for $H + CH_2O$ and 3.9 kcal/mol for $D + H_2CO$ [12].

It is concluded that the present calculations give energetics for the CH_3O system which are of chemical accuracy (in this case the estimated error bars are $\pm$ 1 kcal/mol). This is in contrast to results obtained by Saebø et al. using Møller-Plesset perturbation theory, where the errors in the computed barrier heights are $\approx$ 6 kcal/mol.

Acknowledgement. SPW was supported by NASA cooperative agreement NCC2-478.

References

[a]Mailing Address: NASA Ames Research Center, Moffett Field, CA 94035.

1. See references in Ref. 2.
2. S. Saebø, L. Radom, and H.F. Schaefer III, J. Chem. Phys., **78**, 845(1983).
3. A. Geers, J. Kappert, F. Temps, and J.W. Wiebrecht, Ber. Bunsenges Phys. Chem., **94**, 1219(1990).
4. M. Page, M.C. Lin, Y. He, and T.K. Choudhury, J. Phys. Chem., **93**, 4404(1989).
5. T.H. Dunning, Jr. and P.J. Hay in Methods of Electronic Structure Theory, H.F. Schaefer III ed., Plenum Publishing, 1977.
6. T.H. Dunning, Jr., J. Chem. Phys., **90**, 1007(1989).
7. C.W. Bauschlicher, Jr., S.R. Langhoff, and S.P. Walch, J. Chem. Phys., **96**, 450(1992)
8. S.R. Langhoff and E.R. Davidson, Int. J. Quantum Chem., **8**, 61(1974).
9. SIRIUS is an MCSCF program written by H.J. Jensen and H. Agren and ABACUS is an MCSCF derivatives program written by T. Helgaker, H.J. Jensen, P. Jørenson, J. Olsen, and P.R. Taylor.
10. H.-J. Werner and P.J. Knowles, J. Chem. Phys., **89**, 5803(1988).
11. P.J. Knowles and H.-J. Werner, Chem. Phys. Lett., **145**, 514(1988).
12. F. Temps, private communication.

Table I. Computed stationary point harmonic frequencies (cm^{-1}), rotational constants (cm^{-1}), bond lengths (Å), and bond angles (degrees).

	CH_3O	$CH_3O \rightarrow CH_2OH$	H-CH_2O	H + CH_2O
ω_1	3216	3261	3190	3174
ω_2	2921	2378	1657	1766
ω_3	1608	1556	1471	1589
ω_4	1471	1101	1220	1213
ω_5	1103	1037	605	
ω_6	997	2254 i	1435 i	
ω_7	3284	3391	3297	3272
ω_8	1491	1159	1281	1304
ω_9	1050	1015	770	
A	5.180	5.718	3.927	9.548
B	0.885	0.929	1.007	1.263
C	0.884	0.900	0.962	1.115
r_{C-H_a}	1.092	1.086	1.094	1.097
r_{C-H_b}	1.122	1.275	1.668	
r_{C-O}	1.412	1.418	1.259	1.226
r_{O-H_b}		1.237	2.292	
$\angle$ H_aCH_a	111.5	119.1	117.1	117.2
$\angle$ H_aCH_b	108.2	117.1	91.2	
$\angle$ H_aCO	111.7	116.5	120.3	121.4
$\angle$ H_bCO	105.3	54.4	102.2	

Table II. Computed energies and zero-point corrections.

	zero-point energy[a]	[4s3p2d1f/3s2p1d] basis Energy[b]	Δ E[c]	[5s4p3d2f/4s3p2d] basis Energy[b]	Δ E[c]
CH_3O	0.03905	-114.84037(-.86976)	0.0	-114.86388(-.89511)	0.0
$CH_3O \rightarrow CH_2OH$	0.03394	-114.78503(-.81666)	30.1	-114.80875(-.84226)	30.0
$H\text{-}CH_2O$	0.03074	-114.79504(-.82416)	23.4	-114.81873(-.84963)	23.3
$H + CH_2O$	0.02806	-114.80390(-.83039)	17.8		

[a] energy in E_H.
[b] energy in E_H. The first energy is for CCI, while the energy given in parenthesis is for CCI + Q and is relative to -114. E_H.
[c] relative energy in kcal/mol. The energies are from CCI +Q (i.e. including a multi-reference Davidson's correction) and include zero-point energy.

Table III. Comparison of computed barrier heights (kcal/mol).

	Saebø et al.[a]	Page et al.[b]	PW[c]	Exp.
$H + CH_2O \rightarrow CH_3O$	12.5	8.0	5.6	5.2[d],6.2[e]
$D + CH_2O \rightarrow CDH_2O$			5.2	3.9[d],4.8[e]
$CH_3O \rightarrow CH_2OH$	36.0		30.1	

[a] Reference 2.

[b] Reference 4.

[c] Present work.

[d] Estimated activation energy from a room temperature rate constant for D + H_2CO, an assumed preexponential factor of 2 x 10^{13} cm^3 mol^{-1} sec^{-1}, and a zero-point energy difference between D + H_2CO and H + H_2CO of $\approx$ 1.3 kcal/mol. Ref. 12.

[e] Estimated threshold energy from an RRKM analysis. Ref. 12.